



# Metal dusting on Alloys 602CA and 800

by F.M.L. Mulaudzi\*†‡, L.A. Cornish\*†, G.A. Slabbert\*†‡, and M.J. Papo†‡

## Synopsis

Metal dusting is a corrosion phenomenon that occurs in strongly carburizing gas atmospheres at elevated temperatures. Reaction kinetics and product characterizations of Alloys 602CA and 800 were examined by scanning electron microscopy with energy dispersive X-ray analysis (SEM-EDX) and X-ray diffraction (XRD). The results showed that Alloy 602CA is more resistant to metal dusting than Alloy 800. Visual examination and SEM surface analysis showed that Alloy 800 suffered metal dusting attack after a relatively short exposure period. The amount of coke deposits increased on Alloy 800 with increased exposure from 96 to 336 hours. X-ray diffraction on the reacted surfaces identified graphite and austenite in both alloys and some iron oxides/spinel for Alloy 800.

## Keywords

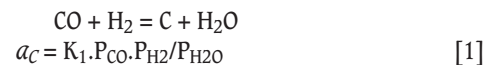
Metal dusting, Alloy 602CA, Alloy 800, SEM-EDX, XRD.

## Introduction

Metal dusting is a severe form of corrosion in which iron, steels, and Ni- and Co-based alloys disintegrate into metal or carbide particles in a coke deposit when exposed to strongly carburizing gases (carbon activity  $a_C > 1$ ) at elevated temperatures (400–800°C)<sup>1</sup>. Chromium-containing alloys can form a protective chromia ( $\text{Cr}_2\text{O}_3$ ) scale to resist metal dusting. However, extensive chromium carbide ( $\text{Cr}_3\text{C}_2$ ,  $\text{Cr}_{23}\text{C}_6$ ) precipitation results in the depletion of chromium to such an extent that the protective chromia scale is not maintained, and therefore metal dusting occurs. The dusting of these alloys is normally in the form of pitting where the original material transforms into a dust of coke or graphite and nanocrystalline-sized oxide particles. The mechanisms leading to metal dusting depend on the substrate material (e.g. Fe, Ni, Ni-based alloys, austenitic, and ferritic steels)<sup>2</sup>. The metal dusting phenomenon occurs in many petrochemical processes and is thus of great significance to the industry because of the cost of replacement of the metal dusted plant components and the associated downtime.

Metal dusting occurs in environments where carbon activity  $a_C > 1$ , and gaseous reactions

that lead to or cause metal dusting are<sup>3</sup>:



## Experimental procedure

The experimental Alloys 602CA and 800 were cut to the dimensions of 2 × 2 cm with a 5 mm hole in the centre for holding a coupon in a ceramic boat. Coupons were ground to a 320 grit finish with SiC paper before exposure in the simulated metal dusting atmosphere in a specially designed rig. For metallographic evaluation, the reacted specimens were first Ni-plated to avoid removal of the surface during preparation, and then mounted in a polyfast conductive resin for scanning electron microscopy (SEM) analysis and in a diallylphthalate for optical microscopy. Mounted specimens were successively ground to 1200 grit using SiC paper, and then polished to 1 μm finish using diamond slurry. Reaction kinetics and product characterizations of both alloys were studied by visual examination, scanning electron microscopy with energy dispersive X-ray analysis (SEM-EDX), and X-ray diffraction (XRD).

The mechanistic studies of metal dusting processes and associated filamentous carbon formation were carried out in Alloys 602CA and 800 under a simulated metal dusting gas

\* School of Chemical and Metallurgical Engineering, University of the Witwatersrand.

† DST/NRF Centre of Excellence in Strong Materials, hosted by the University of the Witwatersrand, Johannesburg.

‡ Advanced Materials Division, Mintek, Randburg.  
© The Southern African Institute of Mining and Metallurgy, 2012. SA ISSN 2225-6253. This paper was first presented at the ZrTa2011 New Metals Development Network Conference, 12–14 October 2011, Mount Grace Country House & Spa, Magaliesburg.

# Metal dusting on Alloys 602CA and 800

Table I  
Nominal composition of Alloy 602CA (wt%)<sup>4</sup>

Cr	Fe	Al	C	Ti	Zr	Y	Ni
25	9.5	2.2	0.18	0.15	0.06	0.08	Bal.

Table II  
Nominal composition of Alloy 800 (wt%)<sup>4</sup>

Cr	Al	C	Ti	Ni	Fe
19–23	0.15–0.6	0.06–0.1	0.15–0.6	30–35	Bal.

mixture (18.9 vol.% CO – 79.1 vol.% H<sub>2</sub> – 2 vol.% H<sub>2</sub>O) at 650°C with carbon activity,  $a_C = 11.75$ , and oxygen partial pressure,  $p_{O_2} = 4.35 \times 10^{-26}$  atm. Alloy 800 is an austenitic iron-based alloy, whereas Alloy 602CA is a nickel-based alloy.

## Results

### Investigation of Alloy 602CA

#### Alloy 602CA before exposure

Figure 1 shows Alloy 602CA before exposure, showing the metallographically prepared surface. An SEM image of the alloy's surface before exposure is shown in Figure 2. Cross-section SEM backscattered electron (BSE) images are shown in Figure 3. There is a dark phase in the matrix, which was shown by EDX analysis to be rich in chromium with small amounts of Ni and Fe. The matrix was found to be rich in Ni and Cr, corresponding to the nominal composition of alloy 602CA. XRD analysis (Figure 4) confirmed the presence of austenite (NiFe).

#### Alloy 602CA after 24 h exposure

Alloy 602CA after 24 hours' exposure is shown in Figure 5. The surface of the alloy turned blue in colour after exposure, but showed no sign of metal degradation. The SEM images in Figure 6 show little change on the surface. The SEM-BSE

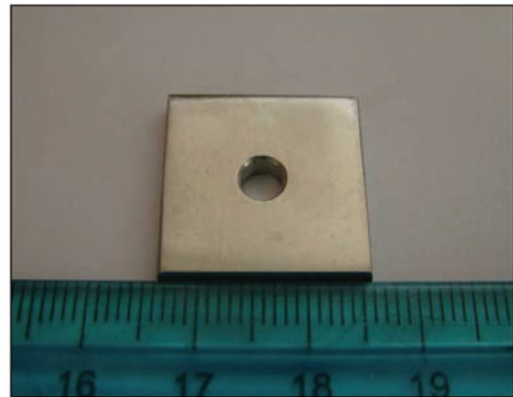


Figure 1—Alloy 602CA before exposure

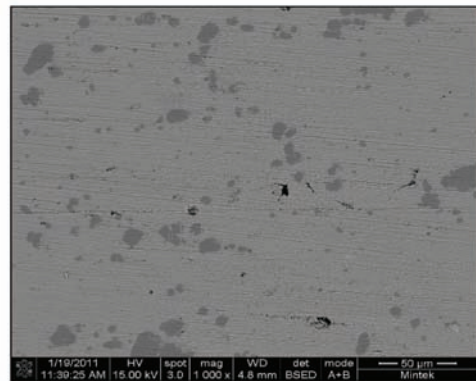
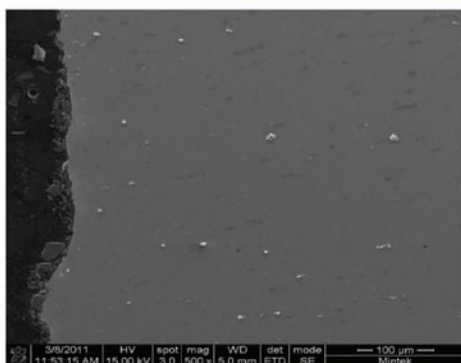


Figure 2—SEM-BSE image of alloy 602CA surface before exposure

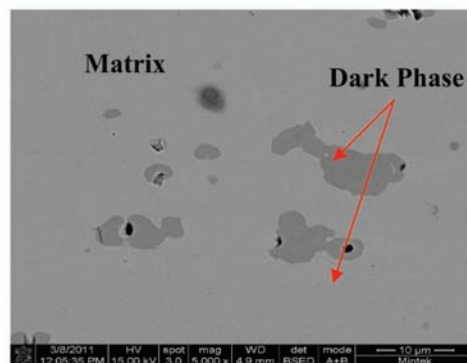
cross-section images in Figure 7 and EDX analysis showed that the dark phase (Figure 7(b)) was rich in chromium and nickel, whereas the matrix was rich in nickel and chromium, with smaller amounts of iron and aluminium. The XRD pattern in Figure 8 confirmed the existence of austenite (FeNi) in the microstructure.

#### Alloy 602CA after 96 h exposure

Figure 9 shows Alloy 602CA after 96 hours' exposure, showing a blue/brown surface of the alloy. The SEM images in Figure 10 show a dark protrusion developing on the



(a)



(b)

Figure 3—SEM-BSE cross-section images of alloy 602CA before exposure

## Metal dusting on Alloys 602CA and 800

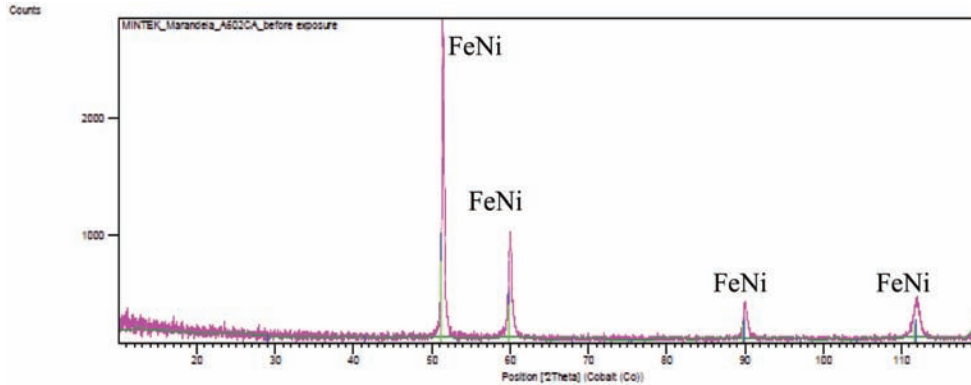


Figure 4—XRD pattern of Alloy 602CA before exposure

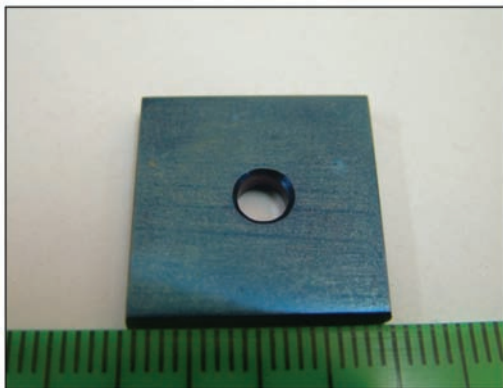


Figure 5—Alloy 602CA after 24h exposure

surface. EDX analysis of the SEM-BSE cross-section revealed the dark phase to be rich in Cr, Ti, and Ni. The alloy matrix, as shown in Figure 11, was rich in nickel and chromium with small amounts of titanium. The overall EDX analyses of the alloy showed the alloy to be rich in Ni, Cr with small amount of Fe. The XRD results still showed the presence of austenite (Figure 12).

### Alloy 602CA after 168 h exposure

Alloy 602CA after 168 hours' exposure showed a bluish/brown colour on the surface, but with no sign of metal degradation, Figure 13. The SEM images of the surface showed some white precipitates, as shown in Figure 14. SEM-BSE cross-section images (Figure 15) showed no sign

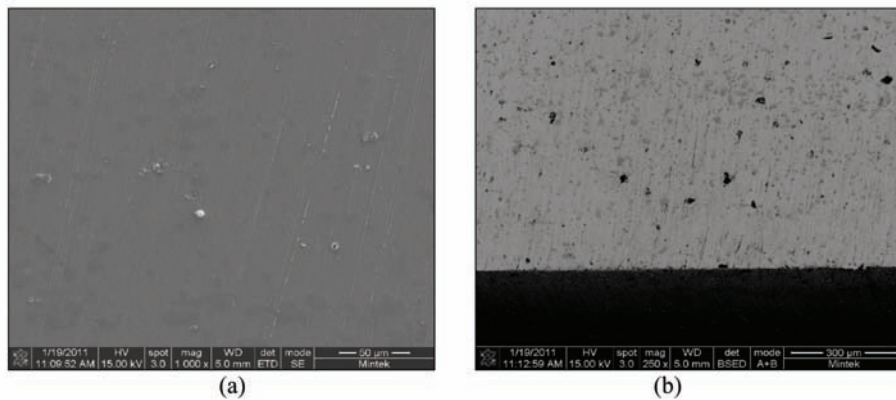


Figure 6—SEM-BSE images of Alloy 602CA surface after 24 h exposure

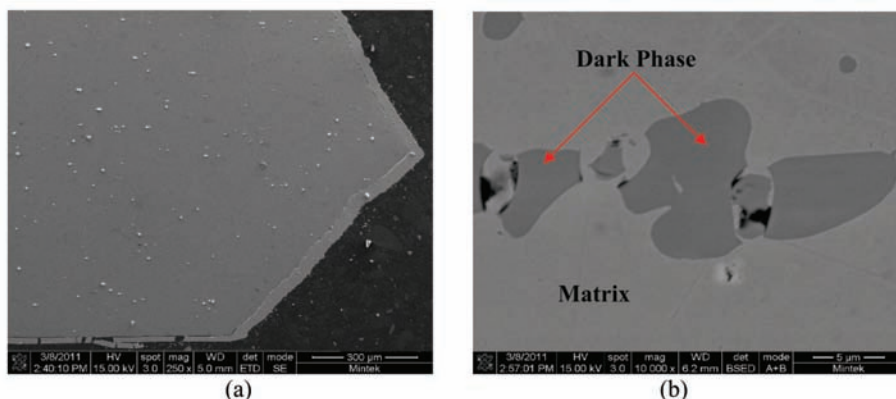


Figure 7—SEM-BSE cross-section images of Alloy 602CA after 24 h exposure



# Metal dusting on Alloys 602CA and 800

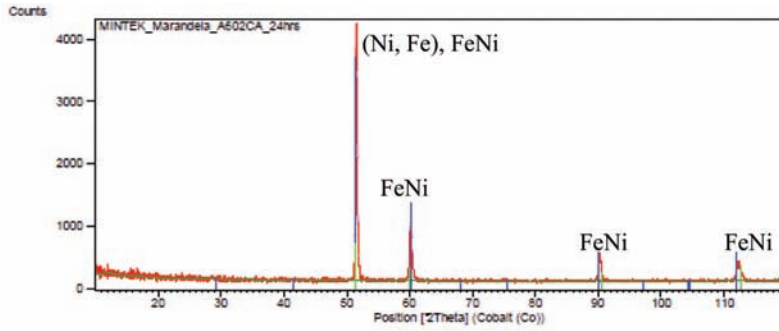


Figure 8—XRD pattern of Alloy 602CA after 24 h exposure

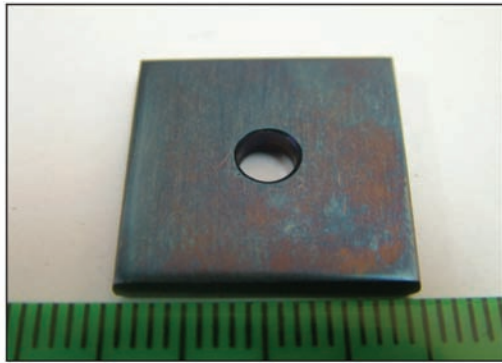


Figure 9—Alloy 602CA after 96 h exposure

of metal dusting attack. EDX analysis revealed that the dark phase was rich in chromium and nickel, and with small amounts of iron and aluminium, whereas the matrix was rich in nickel, chromium, and small amounts of iron and aluminium. XRD showed the existence of the FeNi/NiFe phases (Figure 16).

### Alloy 602CA after 336h exposure

Visual examination of photographic image of Alloy 602CA after 336 hours' exposure showed a small amount of graphite/coke deposits on the surface, as seen in Figure 17, but there was still no sign of metal dusting attack. Figure 18 shows SEM images where the formation of filamentous

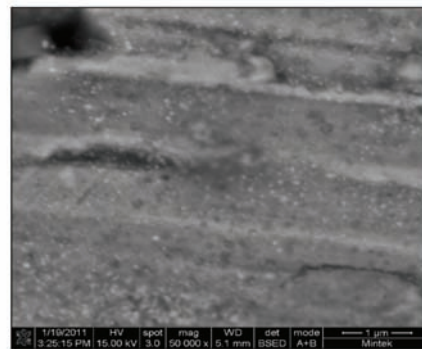
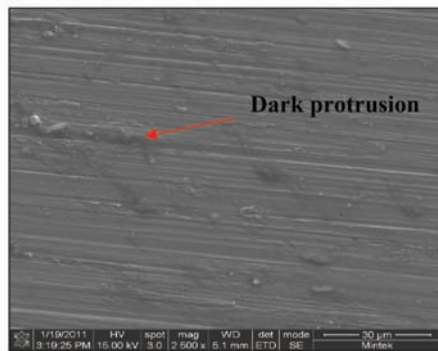


Figure 10—SEM-BSE images of Alloy 602CA surface after 96 h exposure

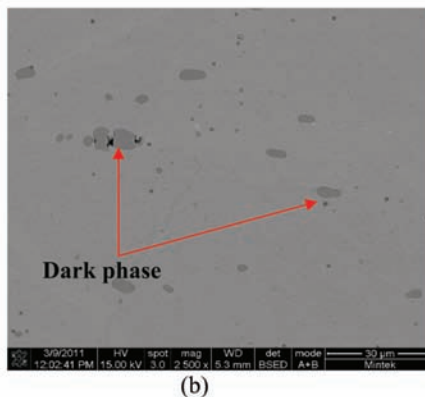
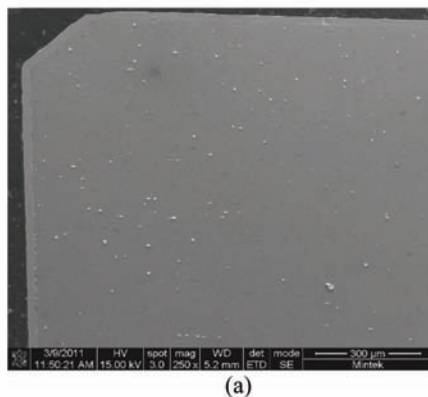


Figure 11—SEM-BSE cross-section images of Alloy 602CA after 96 h exposure

## Metal dusting on Alloys 602CA and 800

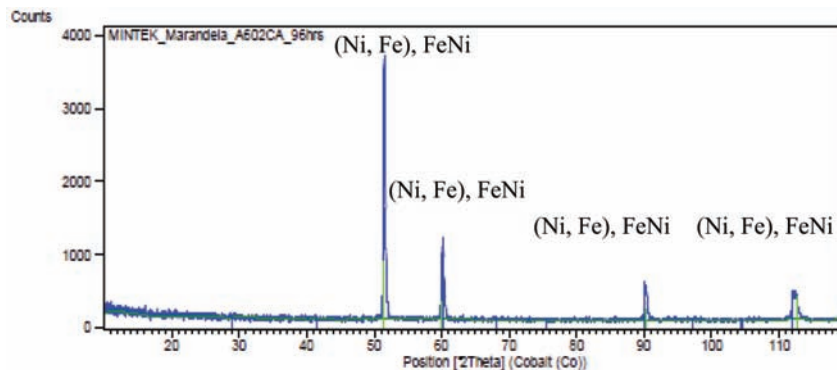


Figure 12—XRD pattern of Alloy 602CA after 96 h exposure

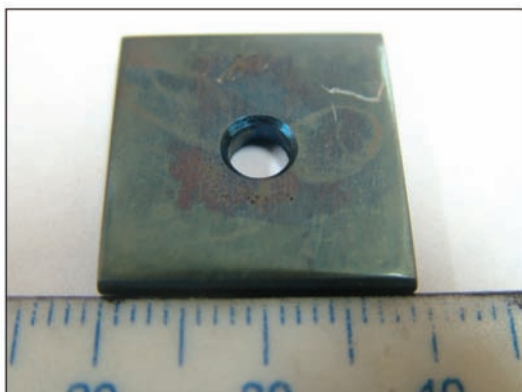


Figure 13—Alloy 602CA after 168 h exposure

carbon is clearly evident on the surface. SEM-BSE cross-section images are given in Figure 19, showing a dark phase and intergranular growth on the alloy. XRD analysis showed the presence of a FeNi phase in the alloy, as shown in Figure 20.

### Investigation of Alloy 800

#### Alloy 800 before exposure

Figure 21 shows Alloy 800 before exposure, with the SEM images in Figure 22 showing an unattacked rough alloy surface. EDX analysis showed the alloy to be rich in iron, nickel, and chromium, and also some titanium. The SEM-BSE cross-section images show a smooth unattacked alloy surface (Figure 23). XRD showed only the presence of FeNi (Figure 24).

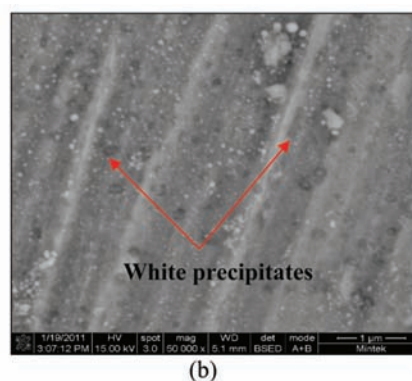
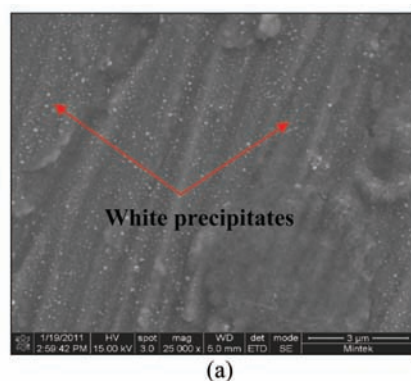


Figure 14—SEM-BSE images of Alloy 602CA surface after 168 h exposure

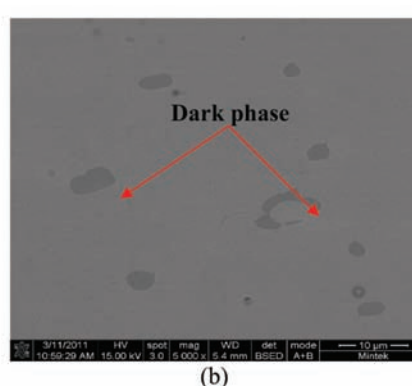
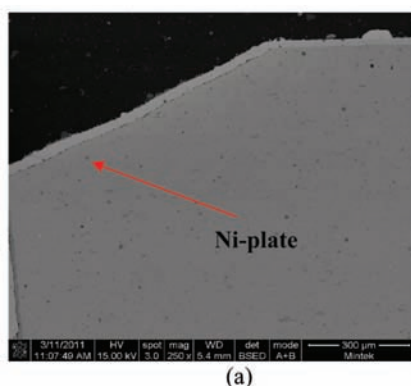


Figure 15—SEM-BSE cross-section images of Alloy 602CA after 168 h exposure

# Metal dusting on Alloys 602CA and 800

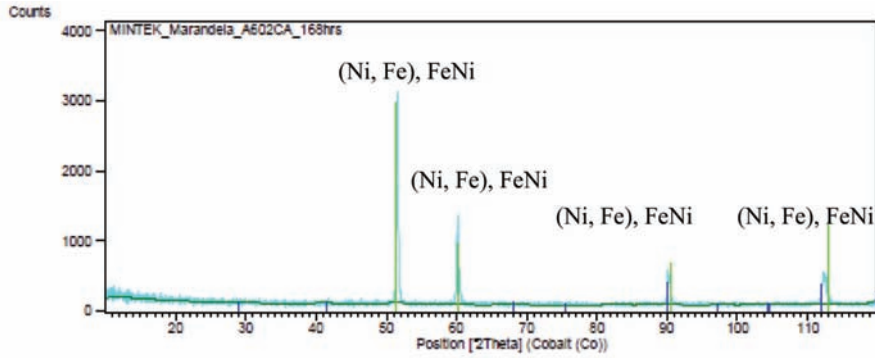


Figure 16—XRD pattern of Alloy 602CA after 168 h exposure

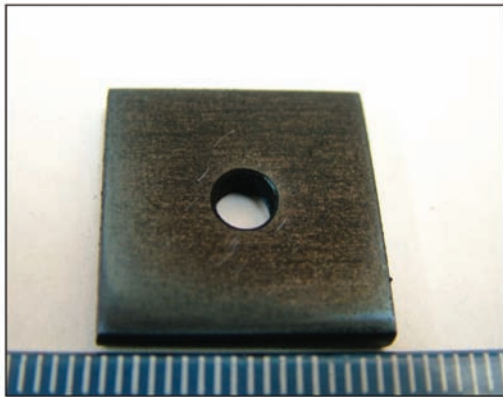


Figure 17—Alloy 602CA after 336 h exposure

### Alloy 800 after 24 h exposure

Alloy 800 after 24 hours' exposure had a purplish/brownish colour on alloy surface (Figure 25). Figure 26 shows uniformly deposited platelets. EDX analysis showed the dark phase to be rich in Ti and Fe, with small amounts of Ni and Cr, whereas the matrix was rich in Fe, Ni, and Cr, with a small amount of Ti. SEM-BSE cross-section images in Figure 27 showed tiny light precipitates. XRD shows the existence of the austenite (FeNi) phase, as given in Figure 28.

### Alloy 800 after 96 h exposure

Alloy 800 after 96 hours' reaction, showed a brownish colour surface with some coke deposits (Figure 29). The SEM images in Figure 30 show uniformly deposited platelets. SEM-BSE cross-section images shown in Figure 31, show

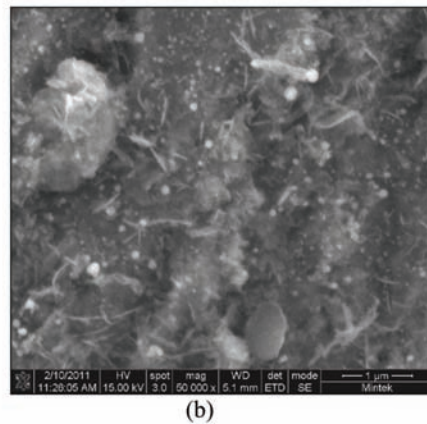
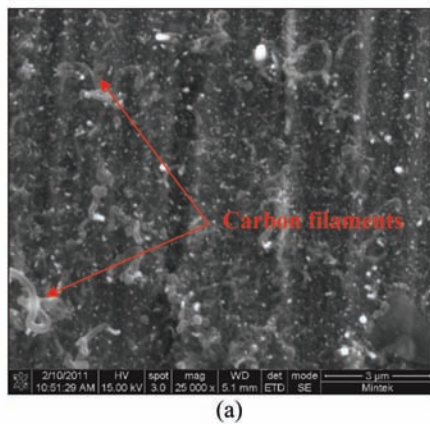


Figure 18—SEM-BSE images of Alloy 602CA surface after 336 h exposure

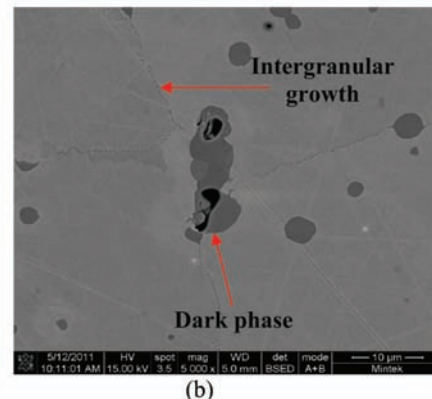
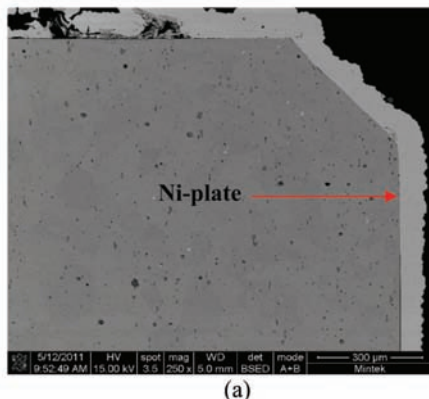


Figure 19—SEM-BSE cross-section images of Alloy 602CA after 336 h exposure



## Metal dusting on Alloys 602CA and 800

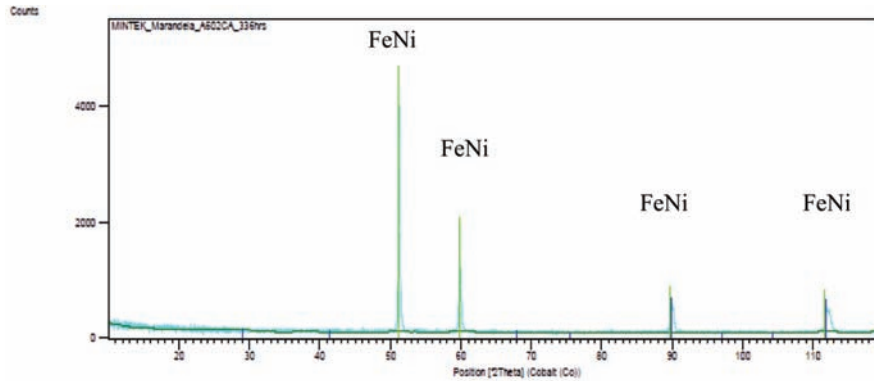


Figure 20—XRD pattern of Alloy 602CA after 336 h exposure

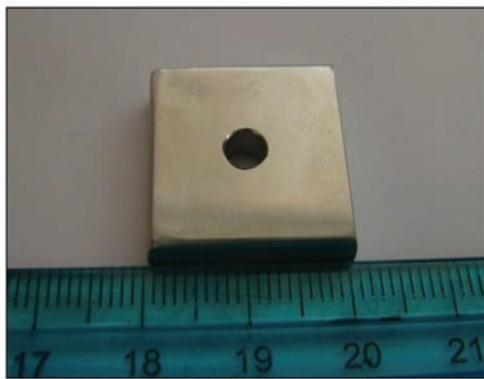


Figure 21—Alloy 800 before exposure

darker phase inclusions, which were found to be rich in titanium and small amounts of iron, chromium and nickel, whereas the matrix was rich in iron, nickel, chromium, and a small amount of titanium. Figure 32 shows the XRD spectrum, indicating the presence of only austenite phase in the alloy.

### Alloy 800 after 168 h exposure

Figure 33 shows Alloy 800 after 168 hours' of reaction where coke deposits were clearly visible on the surface. A high amount of uniformly deposited platelets are seen in SEM images in Figure 34. Figure 35 shows cross-section images with a dark phase in the matrix. EDX analysis showed that the dark phase was rich in titanium with oxygen, iron,

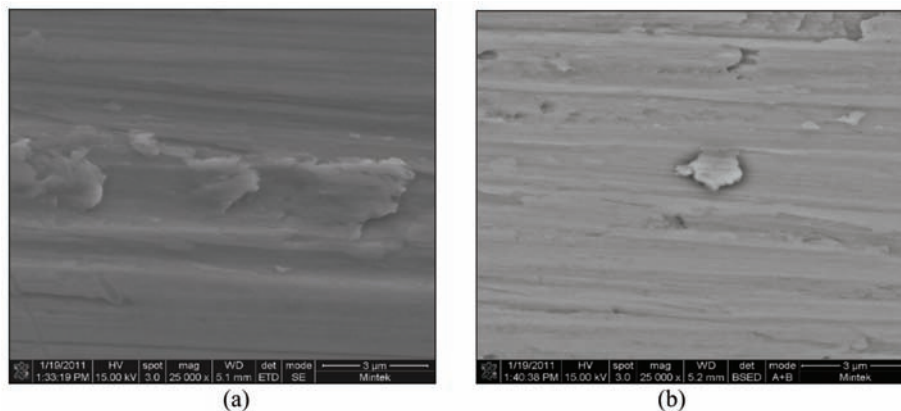


Figure 22—SEM-BSE images of Alloy 800 surface before exposure

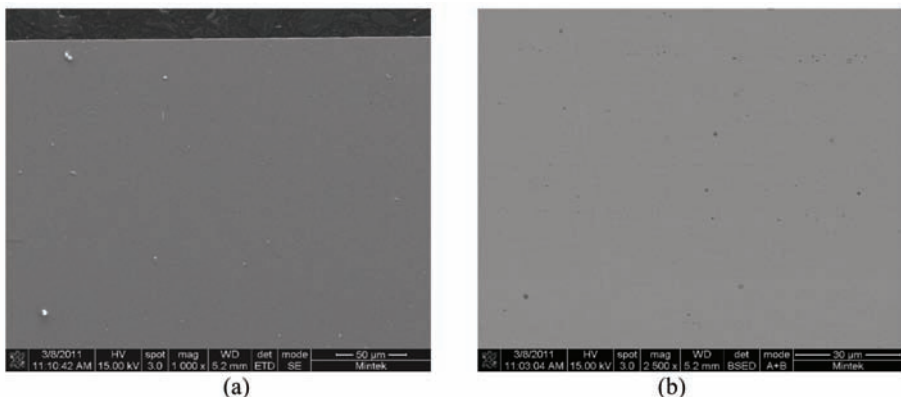


Figure 23—SEM-BSE cross-section images of Alloy 800 before exposure

# Metal dusting on Alloys 602CA and 800

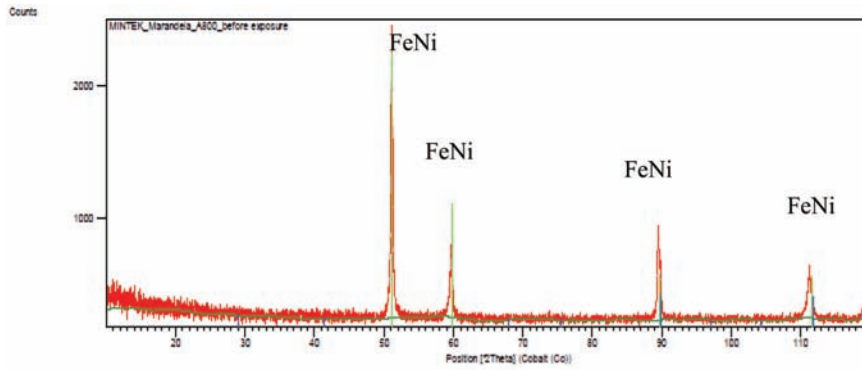


Figure 24—XRD pattern of Alloy 800 before exposure

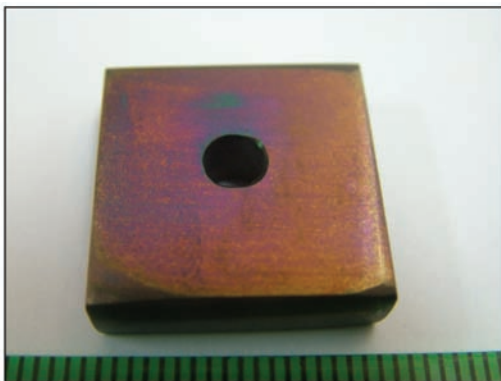


Figure 25—Alloy 800 after 24 h exposure

chromium, and nickel. The Ni-plating was not as uniform as in Figures 31 (a) and (b) because of the attack. The alloy showed some slight metal attack at the edge as shown in Figure 35 (a). The matrix was rich in iron, nickel, and chromium, with small amounts of aluminium, titanium, and manganese. The XRD pattern in Figure 36 showed the presence of both FeNi and Fe<sub>2</sub>O<sub>3</sub>.

### Alloy 800 after 336 h exposure

Alloy 800 after 336 hours' exposure showed increased coke deposit on the surface, as shown in Figure 37. The SEM images in Figures 38(a) and (b) show high amounts of uniformly deposited platelets on the surface, together with some white precipitates. SEM-BSE cross-section images,

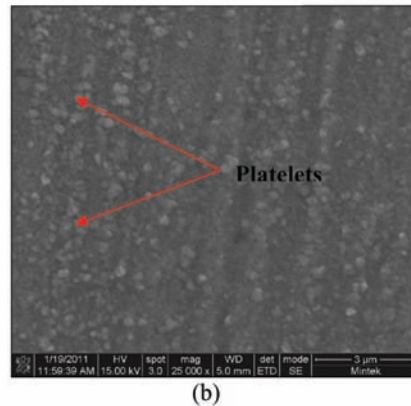
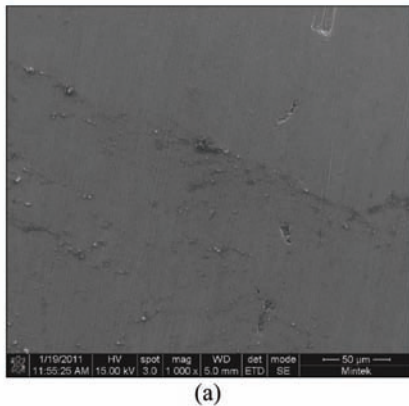


Figure 26—SEM-BSE images of Alloy 800 surface after 24 h exposure

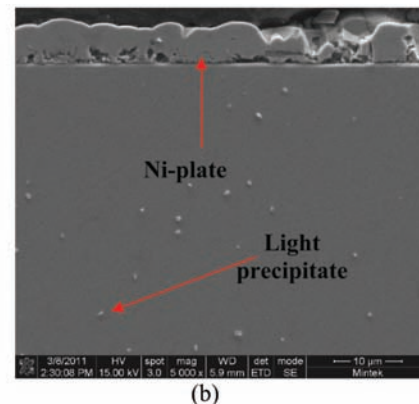
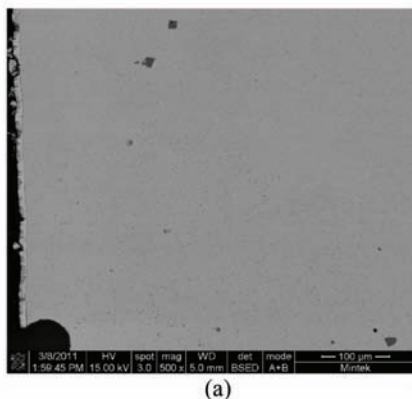


Figure 27—SEM-BSE cross-section images of Alloy 800 after 24 h exposure



## Metal dusting on Alloys 602CA and 800

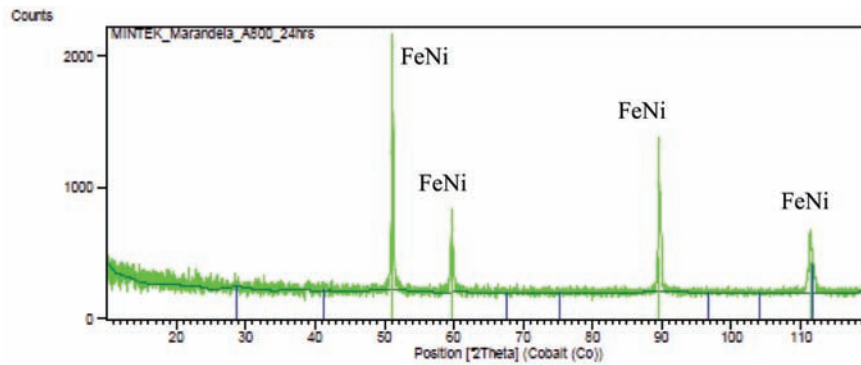


Figure 28—XRD pattern of Alloy 800 after 24 h exposure

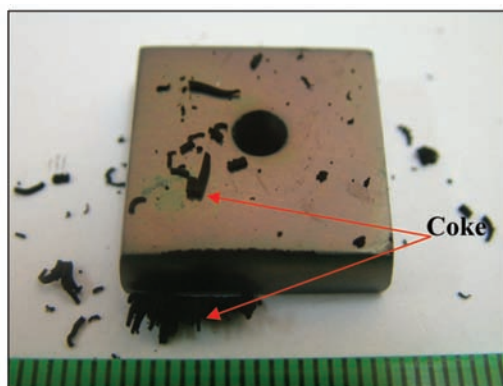


Figure 29—Alloy 800 after 96 h exposure

Figure 39 shows an attacked edge along the Ni-plated layer and also a dark phase with an intergranular growth. XRD of the coke deposits in Figure 40 shows the presence of (Fe, Ni),  $Fe_3O_4$ , and graphite-2H; C, whereas XRD of alloy gave austenite (FeNi) (Figure 41).

### Discussion

The investigation showed that Alloy 602CA is more resistant to metal dusting than Alloy 800. Composition is found to play a vital role in resistance to metal dusting attack, with Alloy 800 being an austenitic Fe-based alloy containing 32Ni, 21Cr and about 0.1C (wt%), whereas Alloy 602CA is a Ni-based alloy containing 25Cr, 9.5Fe, 2.2Al, and 0.18C (wt%). Alloy 602CA can therefore form a double barrier

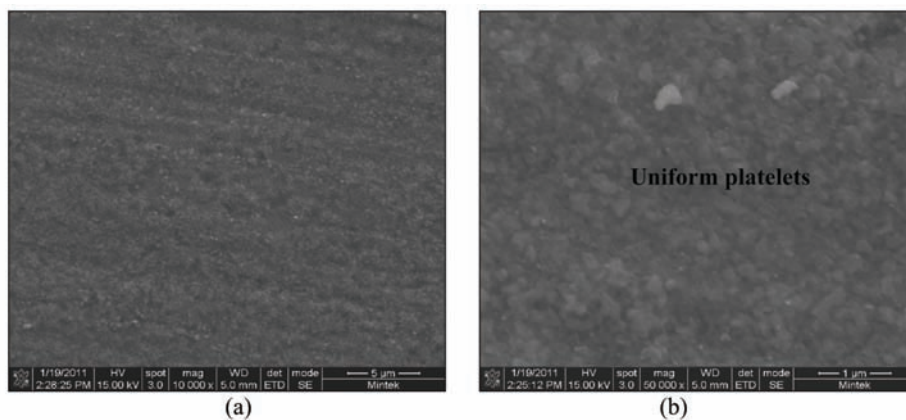


Figure 30—SEM-BSE images of Alloy 800 surface after 96 h exposure

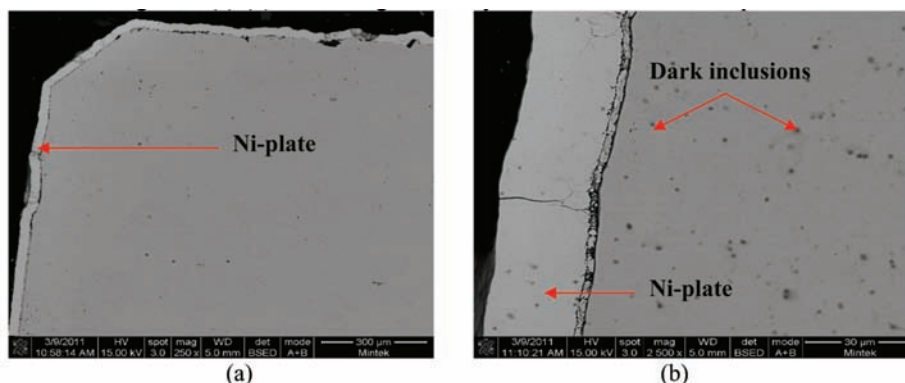


Figure 31—SEM-BSE cross-section images of Alloy 800 after 96 h exposure

# Metal dusting on Alloys 602CA and 800

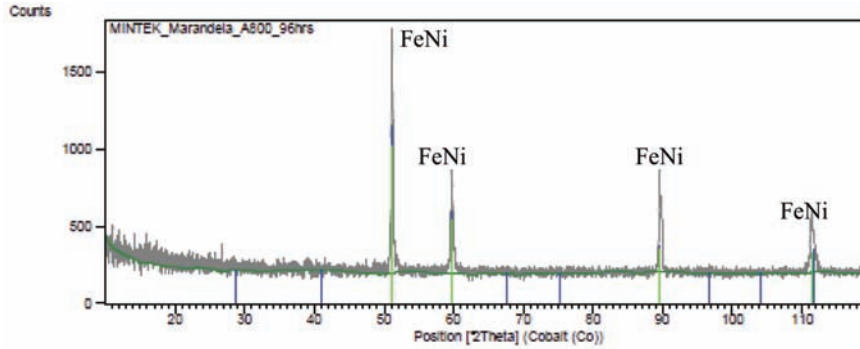


Figure 32—XRD pattern of Alloy 800 after 96 h exposure

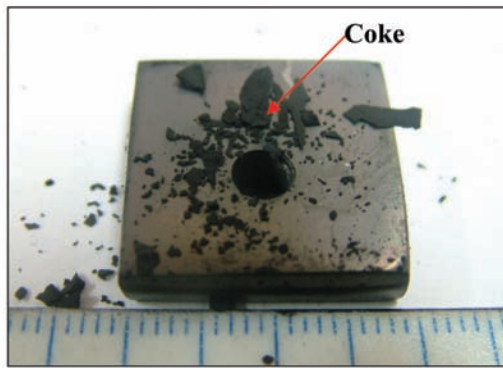
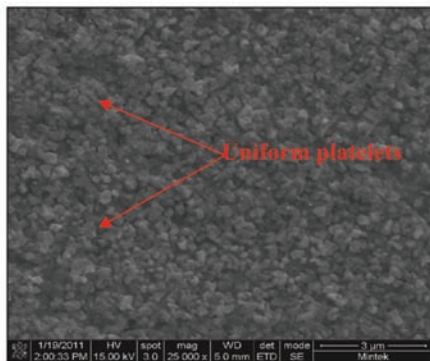


Figure 33—Alloy 800 after 168 h exposure

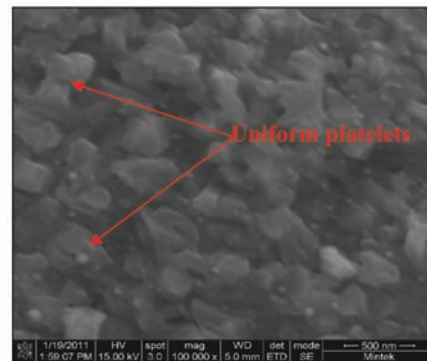
(Cr<sub>2</sub>O<sub>3</sub> and Al<sub>2</sub>O<sub>3</sub>) protective oxide scale, while Alloy 800 can form a Cr<sub>2</sub>O<sub>3</sub> oxide layer, which is another reason why Alloy 800 may have been attacked earlier than Alloy 602CA. Only carbon filaments formed on Alloy 602CA's surface after 336 hours, whereas on Alloy 800 showed increased formation of coke deposits. Alloy 800 had platelets on its surface, which formed in increasing amounts with increased exposure. Platelets are anticipated to be formed by carbon deposits on the alloy's surface, resulting in coke/graphite formation.

### Conclusions

After visual examination, SEM-EDX microanalysis and XRD analysis, the following conclusions were drawn:

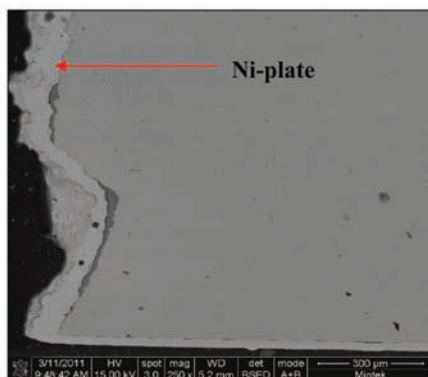


(a)



(b)

Figure 34—SEM-BSE images of Alloy 800 surface after 168 h exposure



(a)



(b)

Figure 35—SEM-BSE cross-section images of Alloy 800 after 168 h exposure

## Metal dusting on Alloys 602CA and 800

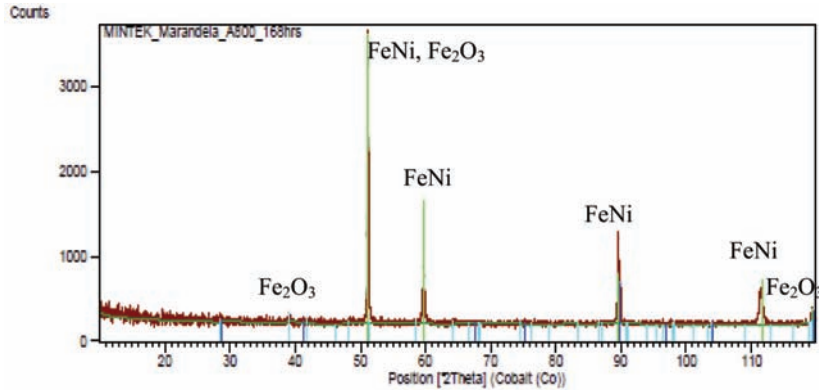


Figure 36—XRD pattern of Alloy 800 after 168 h exposure

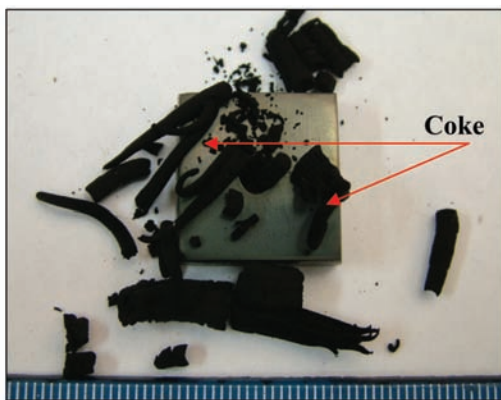


Figure 37—Alloy 800 after 336 h exposure

- Alloy 602CA was found to have greater resistance to metal dusting attack than Alloy 800.
- Alloy 800 suffered metal dusting attack after a relatively short exposure period (96 hours).
- Increasing amounts of coke deposits were formed on Alloy 800 with increased exposure.
- Alloy 602CA was found to contain a grey phase which is rich in chromium and titanium with a small amount of aluminium. Aluminium and chromium are good protective oxide scale formers.
- XRD showed Alloy 602CA to have a common austenite FeNi/NiFe phase, whereas Alloy 800 has a complex phase mix comprising FeNi, Fe<sub>2</sub>O<sub>3</sub>, F<sub>3</sub>O<sub>4</sub>, and graphite-2H; C after metal dusting attack.

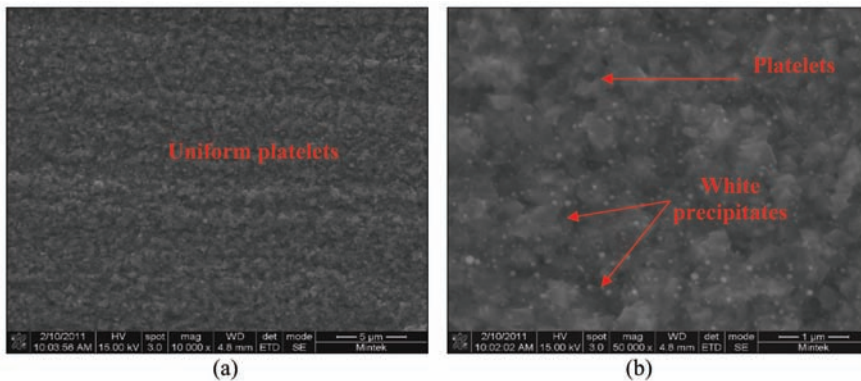


Figure 38—SEM-BSE images of Alloy 800 surface after 336 h exposure

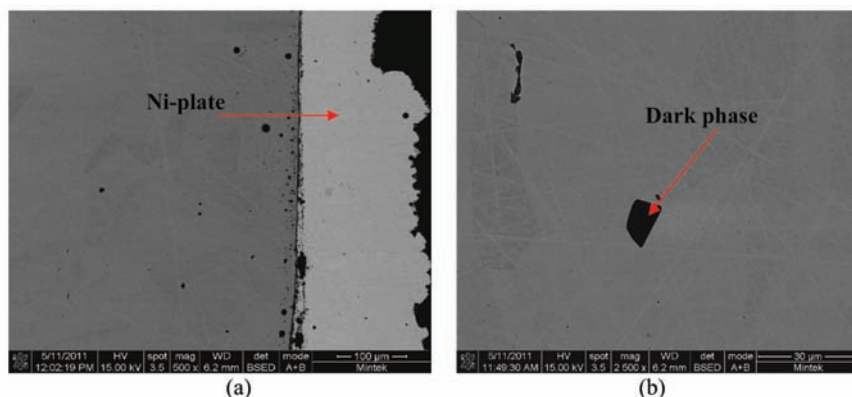


Figure 39—SEM-BSE cross-section images of Alloy 800 after 336 h exposure



## Metal dusting on Alloys 602CA and 800

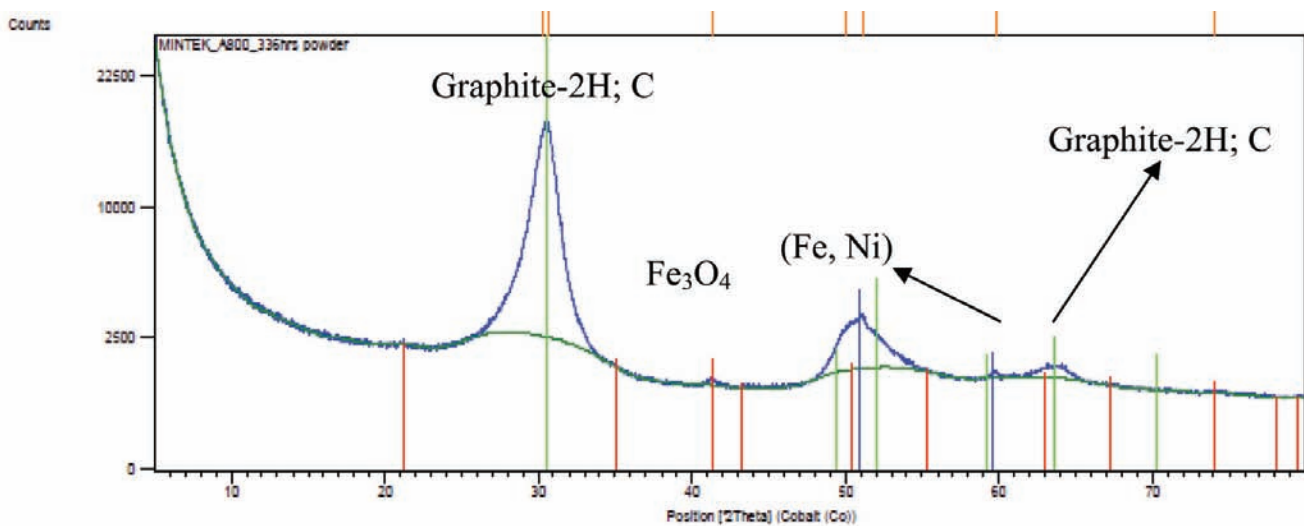


Figure 40—XRD pattern of coke/graphite deposit in Alloy 800 after 336 h exposure

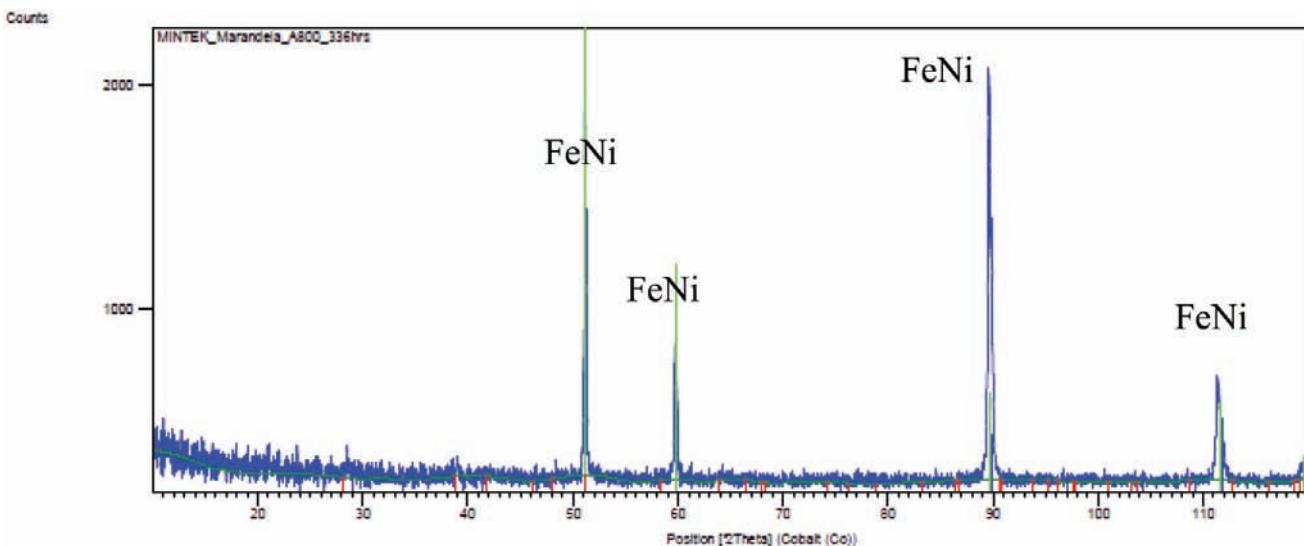


Figure 41—XRD pattern of Alloy 800 after 336 h exposure

### Acknowledgements

This paper is published with the permission of Mintek. The assistance of Mintek, and Department of Science and Technology (DST) through RPDP and FMDN is gratefully acknowledged. L.A. Cornish also thanks the National Research Foundation.

### References

- ZHANG, J., SCHNEIDER, A. and INDEN, G. Characterisation of the coke formed during metal dusting of iron in CO-H<sub>2</sub>-H<sub>2</sub>O gas mixtures. *Corrosion Science*, vol. 45, 2003. pp. 1329–1341.
- RÖHNERT, D., PHILLIPP, F., REUTHER, H., WEBER, T., WESSEL, E., and SCHÜTZE, M. Initial stages in the metal-dusting process on Alloy 800, *Oxidation of Metals*, vol. 68, 2007. pp. 271–293.
- GRABKE, H.J. and SCHÜTZE, M. Corrosion by Carbon and Nitrogen (Metal dusting, Carburization and Nitridation). Woodhead Publishing, Cambridge, UK, 2007.
- HAN, G.W., FENG, D., and DENG, B. Metal dusting and coking of Alloy 803, *Corrosion Science*, vol. 46, 2004. pp. 443–452. ◆